Available online at www.sciencedirect.com
ScienceDirect
Journal of the European Ceramic Society 31 (2011) 1285–1291
www.elsevier.com/locate/jeurceramsoc

Phase diagram of the Al_2O_3–HfO_2–Y_2O_3 system

S.M. Lakiza*, Ja.S. Tyschenko, L.M. Lopato

Frantsevich Institute for Problems of Materials Science, Krzizanovsky 3, 03142 Kyiv, Ukraine

Available online 3 July 2010

Abstract

The phase diagram of the Al_2O_3–HfO_2–Y_2O_3 system was first constructed in the temperature range 1200–2800 °C. The phase transformations in the system are completed in eutectic reactions. No ternary compounds or regions of appreciable solid solution were found in the components or binaries in this system. Four new ternary and three new quasibinary eutectics were found. The minimum melting temperature is 1755 °C and it corresponds to the ternary eutectic $Al_2O_3 + HfO_2 + Y_3Al_5O_{12}$. The solidus surface projection, the schematic of the alloy crystallization path and the vertical sections present the complete phase diagram of the Al_2O_3–HfO_2–Y_2O_3 system.
© 2010 Elsevier Ltd. All rights reserved.

Keywords: Phase diagram; Al_2O_3; HfO_2; Y_2O_3

1. Introduction

The investigation of the Al_2O_3–HfO_2–Y_2O_3 phase diagram is the part of systematic investigation of ternary phase diagrams including alumina, hafnia and oxides of lanthanides. These systems are analogous to the systems Al_2O_3–ZrO_2–Y_2O_3, whose materials are promising as TBC, SOFC, high-temperature structural and functional materials, etc. Hafnia and zirconia are known for their high melting temperatures (2810 and 2710 °C, accordingly), high chemical stability, low thermal conductivity. Hafnia as against zirconia possesses higher chemical stability that allows using its materials at low oxygen pressure and higher vacuum. Thermal expansion of pure and stable HfO_2 is lower, than zirconia, so one can design thermal shock resistant materials.[1] Cubic HfO_2-based solid solutions over 1200 °C possess higher ionic and lower electron conductivity than corresponding ZrO_2-based solid solutions. It makes them promising as high-temperature electrolytes that are in addition more aging stable then materials in the system ZrO_2–Y_2O_3. By partial replacement of Zr^{4+} ions for Hf^{4+} in stable solid solutions one can get cheaper materials, then on the base of expensive hafnia. So systems Al_2O_3–$Zr(Hf)O_2$–Y_2O_3 are perspective for creating oxygen sensors, electrochemical oxygen pumps, heating elements, crucibles for active metals evaporation etc. The Al_2O_3–HfO_2–Ln_2O_3 systems should contain new ternary and binary eutectics which are perspective as structural high-temperature oxide ceramic materials by directional solidification.[2]

The phase diagrams of the bounding binary systems have been examined in some detail.[3–16] The Al_2O_3–HfO_2 system is of the eutectic type with eutectic coordinates 33%[1] HfO_2, 1890 °C and is described elsewhere.[3] The Al_2O_3–Y_2O_3 system[4–10] includes three congruently melting at 1950, 1925 and 1980 °C compounds $Y_3Al_5O_{12}$ (Y_3A_5), $YAlO_3$ (YA) and $Y_4Al_2O_9$ (Y_2A) with corresponding eutectics: $Al_2O_3 + Y_3A_5$ (1825 °C, 19% Y_2O_3), $Y_3A_5 + YA$ (1900 °C, 44% Y_2O_3), $YA + Y_2A$ (1900 °C, 56% Y_2O_3), $Y_2A + Y_2O_3$ (1930 °C, 70.5% Y_2O_3). The system HfO_2–Y_2O_3 is one of the eutectic type with eutectic coordinates 2410 ± 25 °C, 84% Y_2O_3.[11–13] We should pay attention to the fact of any superstructure phase detection in solid state in the system; although in the system ZrO_2–Y_2O_3 superstructure phase $Zr_3Y_4O_{12}$ was found.[14]

Systematic information about the interaction in the system Al_2O_3–HfO_2–Y_2O_3 is absent in the literature. Using XRD data authors[15] constructed isothermal sections at 1600 and 1800 °C. Five three-phase ($M + F(7.5Y_2O_3) + Al_2O_3(AL)$, $F(17Y_2O_3) + AL + Y_3A_5$, $F(38.5Y_2O_3) + Y_3A_5 + YA$, $F(42.5Y_2O_3) + YA + Y_2A$, $F(49Y_2O_3) + C(77.5Y_2O_3) + Y_2A$) and five corresponding two-phase regions that separate indicated three-phase regions were found (M and F – monoclinic (M) and cubic fluorite-like (F) forms of HfO_2, C – cubic

* Corresponding author.
E-mail address: sergij_lakiza@ukr.net (S.M. Lakiza).

[1] In the article concentrations are given in mol.%.

0955-2219/$ – see front matter © 2010 Elsevier Ltd. All rights reserved.
doi:10.1016/j.jeurceramsoc.2010.04.041

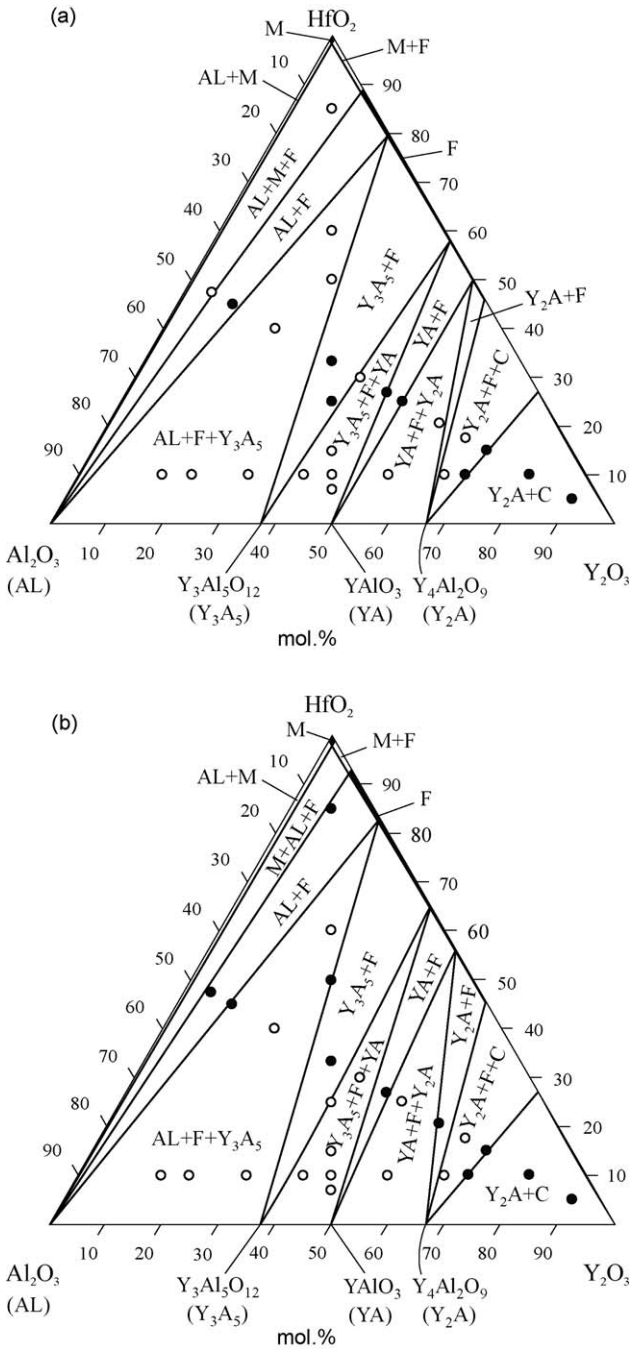

Fig. 1. Isothermal sections of the Al_2O_3–HfO_2–Y_2O_3 phase diagram at: a −1250 °C; b −1650 °C: (●) two-phase samples; (◯) three-phase samples.

form of Y_2O_3). Phase equilibria at both temperatures do not differ within experimental error. In[16] a computer simulation of the Al_2O_3–HfO_2–Y_2O_3 liquidus surface using a CALPHAD method based on experimental results on bounding binaries was done.

In this investigation the Al_2O_3–HfO_2–Y_2O_3 phase diagram is presented as isothermal sections at 1250 and 1650 °C, liquidus and solidus projections on the concentration triangle, schematic of the reactions proceeding during equilibrium crystallization of melted samples and three isopleths in a wide range of temperatures and concentrations.

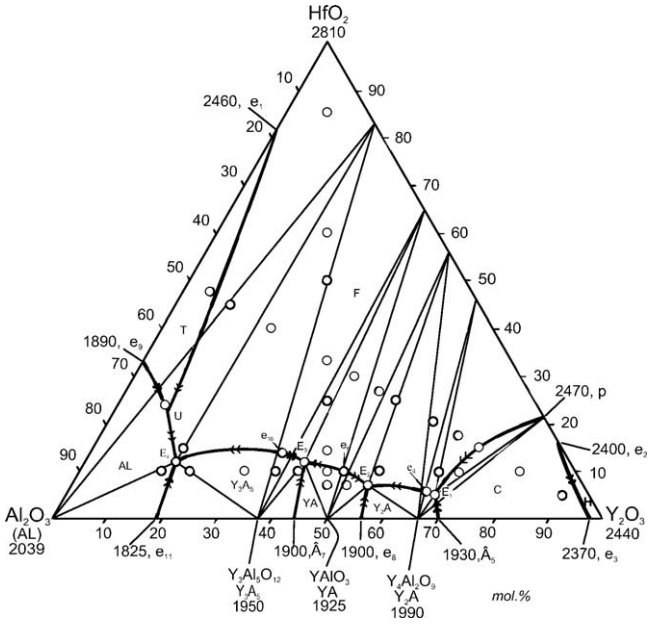

Fig. 2. Projection of the liquidus surface for the Al_2O_3–HfO_2–Y_2O_3 phase diagram.

The analysis of interaction in the binaries Al_2O_3–HfO_2 and HfO_2–Y_2O_3[3,13] discovers their similarity to the binaries Al_2O_3–ZrO_2 and ZrO_2–Y_2O_3.[17] It allowed to assume that the interaction in the system Al_2O_3–HfO_2–Y_2O_3 should be similar to the interaction in the system Al_2O_3–ZrO_2–Y_2O_3 and determined by the structure of bounding systems in the absence of ternary compounds and appreciable solubility areas. In this case the interaction in the ternary system consists in equilibria of binary compounds Y_3A_5, YA and Y_2A with solid solutions F as well as with component oxides and phases on their base. Triangulation of the system should be realized using Y_3A_5–F, YA–F and Y_2A–F sections.

2. Experimental details

Specimens were obtained by both chemical method and melting the component oxides. Powders of $Al(NO_3)_3{\cdot}9H_2O$, $HfO(NO_3)_2{\cdot}2H_2O$ with purity 99.9% (Donetskij zavod khimreaktiviv, Donetsk) and yttria (99.99%) were used for chemical route preparations. Both salts and yttria were dissolved in water with some droplets of concentrated nitric acid added, dried, calcined at 900 °C in air and pressed into pellets 5 mm in diameter and 5 mm in height. Powders of alumina (99.9%), hafnia (99.95%), yttria (99.99%) from Donetskij zavod khimreaktiviv, Donetsk, were used as raw materials. The appropriate quantities of oxides were blended in an agate mortar with ethanol, dried and pressed into pellets of the same dimentions.

Compositions of experimental samples are seen in the corresponding figures. Additional compositions were chosen in the process of identifying the location of the ternary eutectic points. For the constructing of isothermal sections chemically derived samples were annealed at 1250 and 1650 °C for the time necessary to attain equilibrium, established by unchanging XRD patterns. Other samples were fired at 1250 °C in air

Table 1
Comparison of invariant point coordinates in the Al_2O_3–HfO_2–Y_2O_3 and Al_2O_3–ZrO_2–Y_2O_3 systems.

Equilibrium points	Temperature (°C)	Composition (mol.%)			Invariant equilibrium
		Al_2O_3	Hf(Zr)O_2	Y_2O_3	
e_4	1940 [1955] (1940)	29.5 [30] (29)	5.5 [5] (7.5)	65 [65] (63.5)	$L \leftrightarrows Y_2A + F$
E_1	1900 [1954] (1910)	28 [29.4] (26)	5 [4.8] (6)	67 [65.8] (68)	$L \leftrightarrows Y_2A + F + C$
e_6	1910 [1884] (1900)	42 [44.4] (40.5)	10 [8] (11.5)	48 [47.6] (48)	$L \leftrightarrows YA + F$
e_{10}	1875 [1873] (1865)	53 [53.1] (49.5)	12 [11.4] (15)	35[34.6](35.5)	$L \leftrightarrows Y_3A_5 + F$
E_2	1855 [1883] (1850)	39 [43] (37)	7 [7.2] (10)	54 [49.8] (53)	$L \leftrightarrows YA + F + Y_2A$
E_3	1855 [1868] (1830)	48 [50.3] (47)	12 [10] (12)	40 [39.7] (41)	$L \leftrightarrows Y_3A_5 + F + YA$
U	1857 [1823] (1745)	68 [68.4] (63)	23 [22.5] (25)	9 [9.1] (12)	$L + T \leftrightarrows F + AL$
E_4	1755 [1756] (1715)	71 [70.9] (65)	12 [12.6] (19)	17 [16.5] (16)	$L \leftrightarrows AL + F + Y_3A_5$

Results of calculations[16] are given in square [ ] brackets. Results on the system Al_2O_3–ZrO_2–Y_2O_3 are given in round ( ) brackets.

for 6 h, then melted in molybdenum pots in a DTA device[18] at total pressure of H_2 about 1.2 atm and annealed below the solidus temperature for 1 h. The specimens were investigated by DTA in H_2 media at temperatures to 2300 °C,[18] X-ray (DRON-1.5, Burevestnik, St.-Petersburg), petrographic (MIN-8 optical microscope, LOMO, St.-Petersburg) and microstructure phase (JEOL JSM-6490LV) analysis. The accuracy for XRD measurement came to ±0.0003 nm, for refractive indexes measured with immerse liquids ±0.003, with alloys ±0.02.

As far as wide area of solid solutions F exists in the binary bounding system HfO_2–Y_2O_3, we used the compositional dependence of lattice parameter a_F to determine conoid triangles coordinates in the system.[19]

3. Results and discussion

Two isothermal sections at 1250 and 1650 °C were constructed incorporating the literature data and the XRD results obtained (Fig. 1). No ternary compounds or regions of appreciable solid solutions were found in the components or binaries except small regions of ternary solid solutions in the HfO_2 corner. They should exist because of limited Al_2O_3 and Y_2O_3 solubility in HfO_2 at elevated temperatures.[3,13] Both isothermal sections are similar and differ only in the width of phase fields. The existence of two-phase regions AL + F, Y_3A_5 + F, YA + F and Y_2A + F makes it possible to accept that triangulating sections of the system Al_2O_3–HfO_2–Y_2O_3 can be located in these regions. As far as phase F is of a variable composition these sections can be estimated as partially quasibinary.[20]

The liquidus surface for the Al_2O_3–HfO_2–Y_2O_3 phase diagram in conjunction with conoid triangles (Alkemade lines) was experimentally constructed for the first time and is shown in Fig. 2. No ternary compounds were found in the ternary system. The liquidus surface is completed by eight primary crystallization fields of F, T, AL, Y_3A_5, YA, Y_2A, C and H phases. Four four-phase nonvariant eutectic equilibria ($L \leftrightarrows Y_2A + F + C$, $L \leftrightarrows YA + F + Y_2A$, $L \leftrightarrows Y_3A_5 + F + YA$, $L \leftrightarrows AL + F + Y_3A_5$), one four-phase nonvariant transformation equilibrium $L + T \leftrightarrows F + AL$ and three three-phase nonvariant eutectic equilibria ($L \leftrightarrows Y_3A_5 + F$, $L \leftrightarrows YA + F$, $L \leftrightarrows Y_2A + F$) were found in the ternary system. As far as HfO_2 interacts with every other phases eutectically, this fact allows to combine in materials the unique properties of HfO_2-based F-phases with the properties of other phases of the Al_2O_3–HfO_2–Y_2O_3 system.

The coordinates of invariant points of the Al_2O_3–HfO_2–Y_2O_3 phase diagram are listed in Table 1. It should be emphasized a very good agreement between the composition of E_4 obtained in this investigation and the results of.[16] The microstructures of the invariant points E_1–E_4 are shown in Fig. 3. The minimum melting temperature in the system is 1755 °C and it relates to the ternary eutectic E_4. The maximum liquidus temperature is 2810 °C and it refers to the melting point of pure HfO_2.

The solidus surface for the Al_2O_3–HfO_2–Y_2O_3 phase diagram was constructed for the first time. The projection of the solidus surface of the Al_2O_3–HfO_2–Y_2O_3 phase diagram is shown in Fig. 4. Data on the coordinates of the conoid triangles of solid phases on the solidus surface were obtained from XRD measurements and are given in Table 2. Solidus surface consists of five isothermal fields which correspond to four invariant eutectic equilibria and one invariant transformation equilibrium. The solidus surface includes also six linear surfaces of binary eutectics crystallization end. The highest solidus temperature in the system is 2810 °C – the HfO_2 melting point, the lowest is

Table 2
Coordinates of the apexes of the solid-phase tie-line triangles on the solidus surface of the Al_2O_3–HfO_2–Y_2O_3 phase diagram.

Phase field	Composition of the equilibrium phases (mol%)						
	AL	T	F	Y_3A_5	YA	Y_2A	C
AL+M+F	100	98,5HfO_2–1,5Y_2O_3	93HfO_2–7Y_2O_3	–	–	–	–
AL+F+Y_3A_5	100	–	83HfO_2–17Y_2O_3	100	–	–	–
Y_3A_5+F+YA	–	–	65HfO_2–35Y_2O_3	100	100	–	–
YA+F+Y_2A	–	–	56HfO_2–44Y_2O_3	–	100	100	–
Y_2A+F+C	–	–	46HfO_2–54Y_2O_3	–	–	100	27,5HfO_2–72,5Y_2O_3

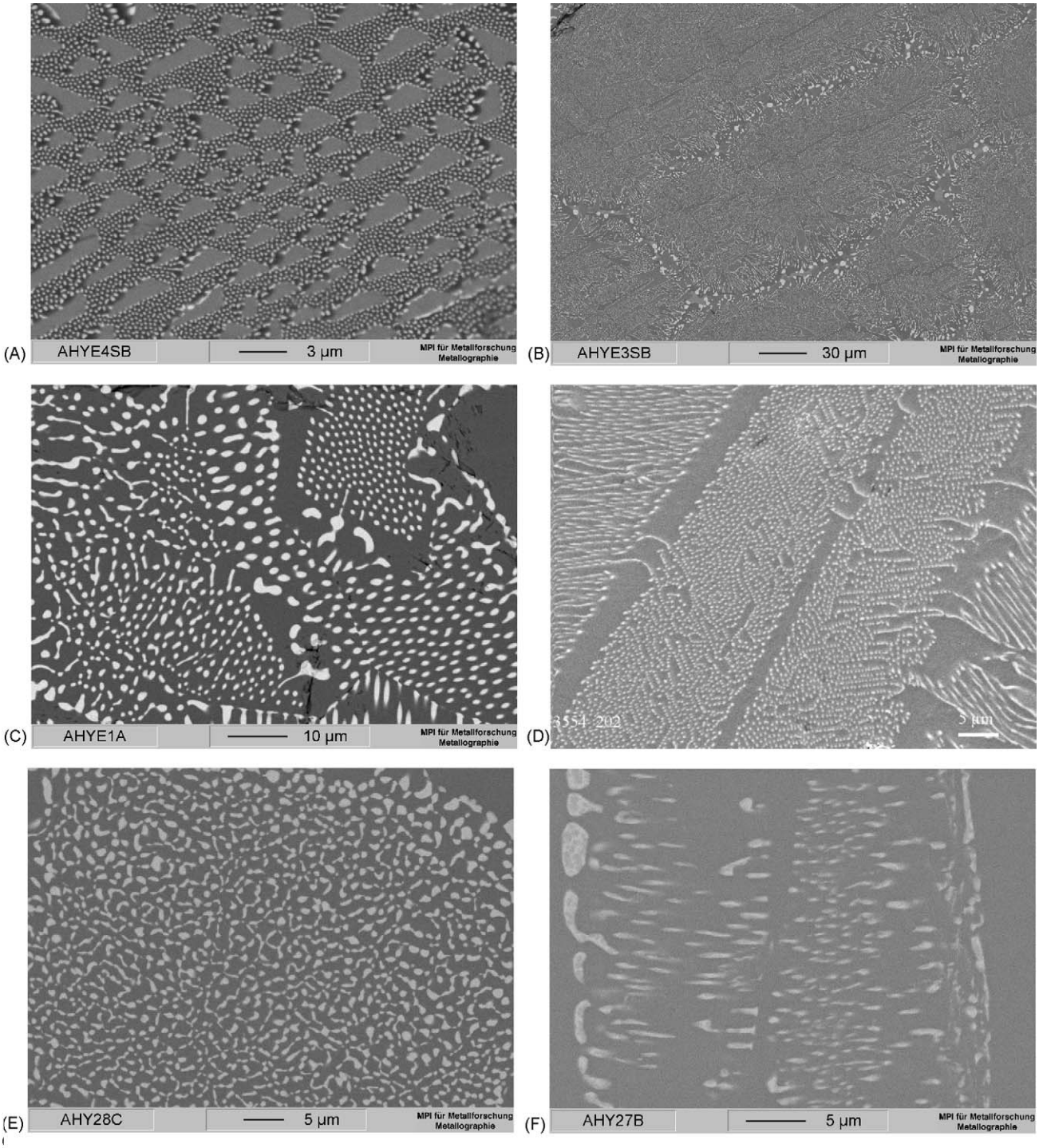

Fig. 3. Microstructures of some alloys in the $Al_2O_3-HfO_2-Y_2O_3$ system, mol%.: A – ternary eutectic point E_4: dark phase – AL, grey phase – Y_3A_5, light phase – F; B – ternary eutectic point E_3: dark phase – Y_3A_5, grey phase – YA, light phase – F; C – ternary eutectic point E_1: dark phase – Y_2A, light small phase – F, light large phase – C; D – saddle point e_{10}: dark phase – Y_3A_5, light phase – F; E – saddle point e_6: dark phase – YA, light phase – F; F – saddle point e_4: dark phase – Y_2A, light phase – F.

1755 °C – the ternary eutectic AL + F + Y_3A_5 melting temperature. No ternary compounds and appreciable third component solubility in components and binary compounds were found in the ternary system.

The diagram of equilibrium alloys crystallization scheme for the Al_2O_3–HfO_2–Y_2O_3 system was constructed using data on bounding binary systems, liquidus and solidus surfaces (Fig. 5). So the equilibrium alloys crystallization in this system is characterized with one invariant four-phase transformation process at 1857 °C (*U*), four invariant four-phase congruent processes at 1900 °C (E_1), 1855 °C (E_2), 1855 °C (E_3) and 1755 °C (E_4) and three invariant three-phase congru-

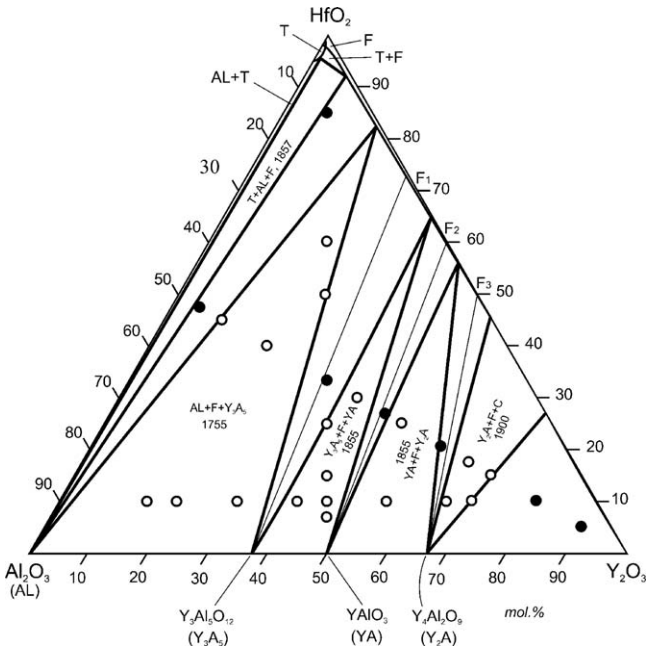

Fig. 4. Solidus surface projection for the Al_2O_3–HfO_2–Y_2O_3 phase diagram: (●) two-phase samples; (◯) three-phase samples.

ent processes at 1940 °C (e_4), 1910 °C (e_6) and 1875 °C (e_{10}) (Fig. 5).

Three polythermal sections were constructed to present the phase diagram of the Al_2O_3–HfO_2–Y_2O_3 system more completely: bisectors $Al_2O_3/HfO_2 = 1$, $Al_2O_3/Y_2O_3 = 1$ and isopleth 10 mol.% HfO_2 (Figs. 6–8). These figures confirm the triangulation and discover the interaction in different parts of the Al_2O_3–HfO_2–Y_2O_3 phase diagram.

The results obtained coincide qualitatively with the results of,[15] but it is necessary to note the absence of narrow two-phase field AL + M adjacent to the boundary Al_2O_3–HfO_2, and narrow areas M, M + F and F in the HfO_2 corner. Experimental determination of these areas is very complicated, but they should be represented in isothermal sections for their correct presentation. In addition in this system we have found ternary eutectic AL + F + Y_3A_5 with coordinates 71% Al_2O_3–12% HfO_2, 1755 °C. Therefore in the samples 17–19 from conoid triangle Al_2O_3–F–Y_3A_5[15] primary F and secondary F + Y_3A_5 crystals with small quantities of eutectic liquid should be present at 1800 °C. As far as authors of[15] did not investigated microstructures of sintered at 1800 °C samples, but grinded them before XRD, so they could not reveal liquid formation

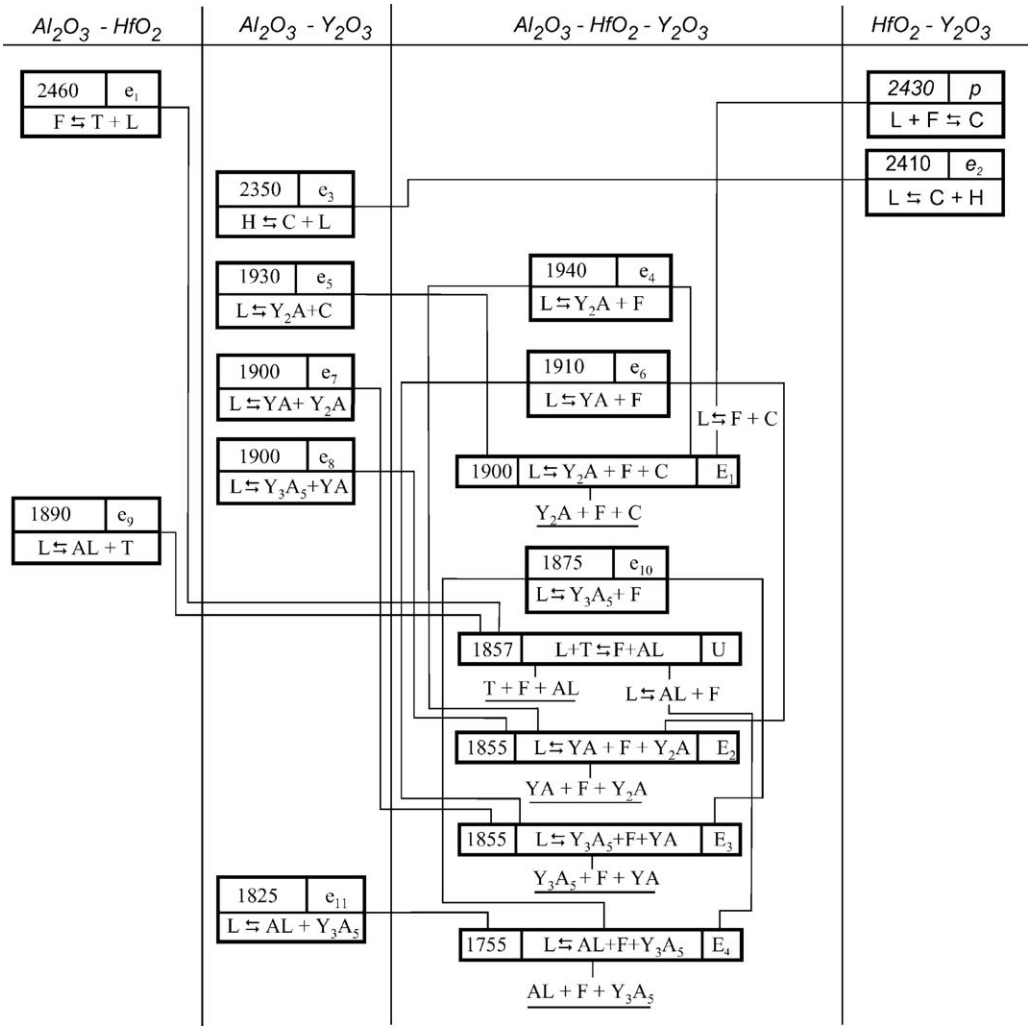

Fig. 5. Schematic of the reactions proceeding during sample crystallization in the Al_2O_3–HfO_2–Y_2O_3 system.

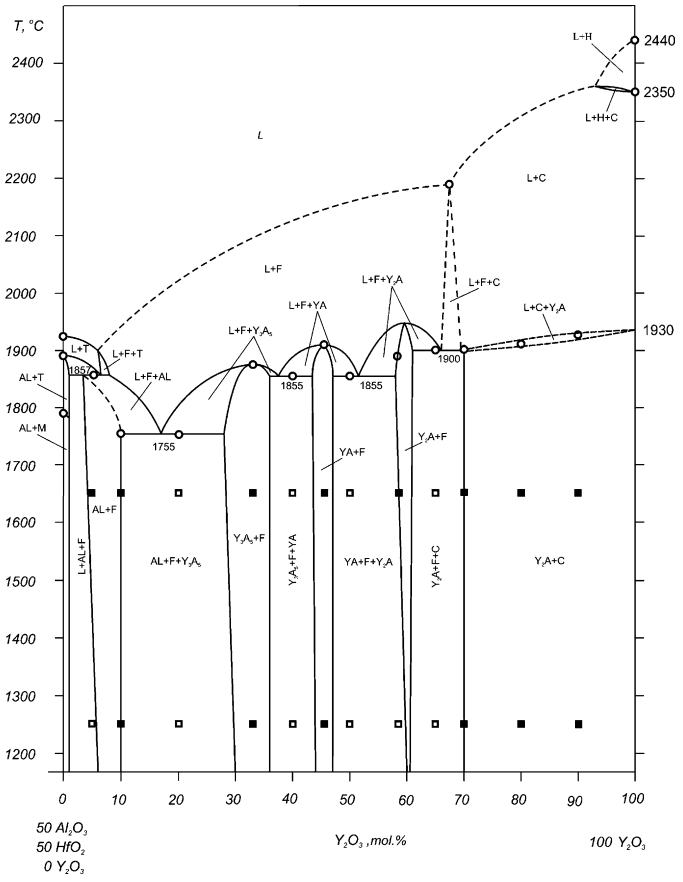

Fig. 6. Bisector $Al_2O_3/HfO_2 = 1$ for the Al_2O_3–HfO_2–Y_2O_3 phase diagram.

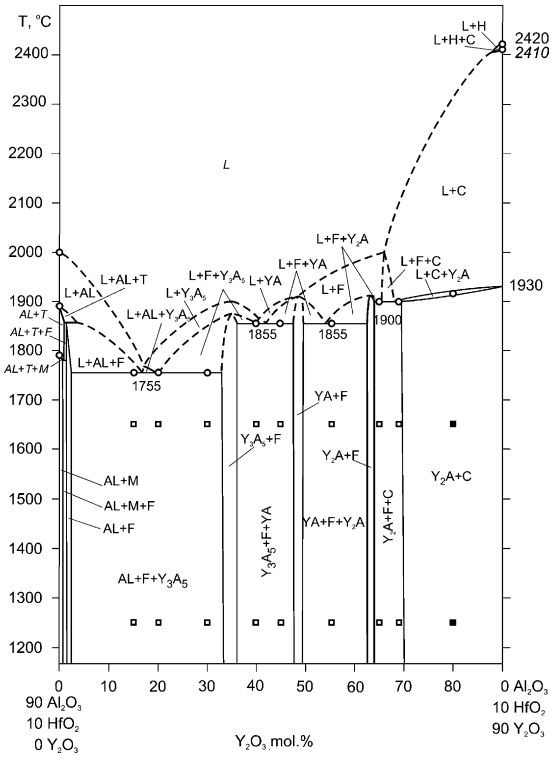

Fig. 7. Bisector $Al_2O_3/Y_2O_3 = 1$ for the Al_2O_3–HfO_2–Y_2O_3 phase diagram.

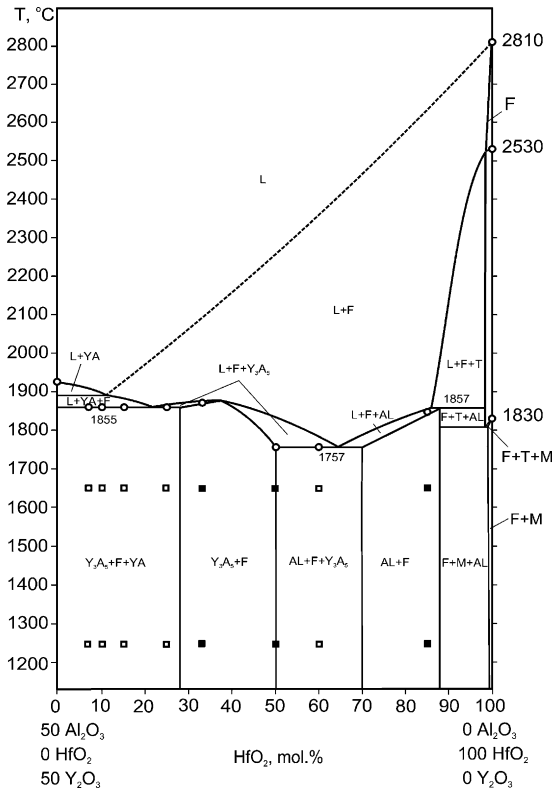

Fig. 8. Isopleth 10 mol% HfO_2 for the Al_2O_3–HfO_2–Y_2O_3 phase diagram.

in them. On other way, samples with compositions, close to the eutectic point were not prepared, so authors could not observe complete sample melting. Therefore isothermal section of the Al_2O_3–HfO_2–Y_2O_3 system, presented in Ref. 15,[15] cannot be related to 1800 °C, but to 1700 °C at most.

Very interesting discrepancy was found between our experimental results and calculations[16] in isothermal section of the system at 1250 °C. According to the calculations there is change of tie lines due to invariant reaction $F + AL \leftrightarrows Y_3A_5 + M$ in solid phases between 1250 and 1600 °C. This fact necessitates additional investigation of this invariant reaction in temperature range 1250–1600 °C to establish real equilibrium in this part of the system. Above 1600 °C experimental and calculated results agree well. At the same time, the results on experimental and calculated liquidus surfaces are in perfect mutual agreement (Table 1).

Comparison of the invariant point coordinates of the system studied and the system-analogue Al_2O_3–ZrO_2–Y_2O_3[17] (Table 1) revealed that the temperatures of invariant points are 5–40 °C higher for the system with HfO_2 and their compositions contain excess of 1–4% HfO_2 and deficit of ~1% Y_2O_3. Such temperature and compositional distinctions can be explained by higher HfO_2 melting point as against ZrO_2.

4. Conclusions

The phase diagram of the Al_2O_3–HfO_2–Y_2O_3 system was constructed in the temperature range 1250–2800 °C. The liquidus surface of the phase diagram reflects the preferentially

eutectic interaction in the system. Four new ternary and three new binary eutectics were found. No ternary compounds or regions of appreciable solid solution were found in the components or binaries in this ternary system. The minimum melting temperature is 1755 °C and it corresponds to the ternary eutectic $Al_2O_3 + F–HfO_2 + Y_3Al_5O_{12}$, maximum melting temperature belongs to the melting of HfO_2. The polythermal sections present the complete phase diagram of the Al_2O_3–HfO_2–Y_2O_3 system.

References

1. Lopato LM, Shevchenko AV, Frolov AA, Red'ko VP. *Poroshkovaya Metalurgiya* 2005;**7/8**:36–42 [in Russian].
2. Lakiza SM. *Poroshkovaya Metalurgiya* 2009;**1/2**:57–77 [in Ukraine].
3. Lopato LM, Shevchenko AV, Gerasimjuk GI. *Izv AN SSSR Neorgan Mater* 1976;**12**(9):1623–6 [in Russian].
4. Toropov NA, Bondar IA, Galahov FJa, Nikogosyan HS, Vinogradova N. *Izv AN SSSR Ser Khim* 1964;**7**:1158–64 [in Russian].
5. Viehnicki D, Schmidt F. *J Mater Sci* 1969;**4**(1):84–8.
6. Caslavsky JL, Viechnicki DJ. *J Mater Sci* 1980;**15**(7):1709–18.
7. Bondar IA, Korol'ova LN, Bezruk ET. *Izv AN SSSR Neorgan Mater* 1984;**20**(2):257–61 [in Russian].
8. Cocayne B. *J Less-Com Met* 1985;**114**(1):199–206.
9. Mah T, Petry D. *J Am Ceram Soc* 1992;**75**(7):2006–9.
10. Lakiza SN, Lopato LM, Nazarenko LV, Zajtceva ZA. *Poroshkovaya Metalurgiya* 1994;**11/12**:39–43 [in Russian].
11. Spiridonov FN, Komissarova LN, Kogarov LU, Spicin VI. *Z Neorgan Khim* 1969;**14**(9):2535–40.
12. Stacy DW, Wilder DR. *J Am Ceram Soc* 1975;**58**(7–8):285–8.
13. Shevchenko AV, Lopato LM, Kirjakova IE. *Izv AN SSSR Neorgan Mater* 1984;**20**(12):1991–4 [in Russian].
14. Scott HG. *J Mater Sci* 1977;**12**(2):311–9.
15. Popov SG, Paromova MV, Kulikova ZJa, Rozanova ON, Pashin SF. *Neorg Mater* 1990;**26**(5):1002–6.
16. Fabrichnaya O, Mercer C. *Comp Coupl Phase Diagr Thermochem* 2005;**29**:239–46.
17. Lakiza SM, Lopato LM. *J Am Ceram Soc* 1997;**80**(4):893–902.
18. Lopato LM, Shevchenko AV, Kuschevsky AE. *Poroshkovaya metalurgiya* 1972;(1):88–92 [in Russian].
19. Lakiza SM, Tyschenko JaS, Red'ko VP, Lopato LM. *Poroshkovaya metalurgiya* 2009;**3/4**:131–40 [in Ukraine].
20. Eremenko VN, Velikanova TJa, Art'uh LV, et al. *Ternary systems of molybdenum with carbon and transition metals from IV group*. Kyiv: Naukova Dumka; 1985, 296 p.